

Spatial Coherence Measurement of Soft X-Ray Radiation Produced by High Order Harmonic Generation

T. Ditmire,¹ E. T. Gumbrell,¹ R. A. Smith,¹ J. W. G. Tisch,¹ D. D. Meyerhofer,² and M. H. R. Hutchinson¹

¹*Blackett Laboratory, Imperial College of Science Technology and Medicine, London SW7 2BZ, United Kingdom*

²*Department of Mechanical Engineering, University of Rochester, Rochester, New York 14627*

(Received 26 July 1996)

We have executed a series of Young's two-slit experiments to measure the spatial coherence of soft x rays produced by high order harmonic generation in helium within the 270 to 480 Å wavelength range. We find that the harmonics exhibit good fringe visibility and high spatial coherence, though the coherence is somewhat degraded at high intensity because of the production of free electrons through optical field ionization during the harmonic generation. [S0031-9007(96)01799-1]

PACS numbers: 42.65.Ky, 42.25.Kb

The extensive research of high order harmonic generation in gases by intense, short laser pulses has been motivated by the potential of using these harmonics as a source of high brightness, coherent, soft x-ray radiation [1]. However, to date, the actual spatial coherence of the harmonics has not been measured. While a number of previous experimental studies have characterized the far field profiles of the high order harmonics [2–4], knowledge of the far field profile alone does not indicate the actual transverse spatial coherence of the radiation. Measuring the transverse coherence requires performing some manner of interference experiment such as a Young's two-slit experiment [5]. Previously, such techniques have been applied to measure the spatial coherence of short wavelength XUV [6] and soft x-ray lasers [7] as well as laser-plasma x-ray sources [8].

The coherence of high order harmonics is expected to be high since such radiation is created by the conversion of coherent, single mode, laser radiation [1]. Measurements of the harmonics' far field profiles have indicated that the harmonics largely preserve the low divergence, Gaussian character of the laser radiation [2–4,9]. However, a more fundamental question is whether the high order harmonics preserve the high spatial coherence of the fundamental laser radiation. Knowledge of the harmonics' coherence is important not only to understand the physics of the harmonic generation process but also important if harmonics are to be used in interferometric applications. In this Letter we report on the first measurement of the transverse spatial coherence of high order harmonic radiation. We have conducted a series of Young's two-slit experiments to measure the spatial coherence of soft x ray, high order harmonics in the 270 to 480 Å wavelength range, produced by a high intensity, 2 ps, 527 nm laser pulse in helium. These harmonics exhibit good fringe visibility and high spatial coherence, though we find that the coherence is somewhat degraded at high intensity because of the production of free electrons through optical field ionization during the harmonic generation. Nonetheless, the harmonics exhibit coherence that is substantially better than the previously reported spatial coherence of soft x-ray lasers [7,10].

In our experiment, harmonics were generated with a Nd:glass laser based on chirped pulse amplification. This laser produces 2 ps pulses at a wavelength of 1054 nm with energy up to 0.5 J. These pulses were frequency doubled in a potassium dihydrogen phosphate crystal to a wavelength of 527 nm, a configuration yielding high conversion efficiency into harmonics in the 200–500 Å range [11]. The Gaussian laser beam spatial profile was apertured prior to the $f/50$ focusing lens to produce a uniform, near flat-top profile. The near diffraction limited pulse was focused into a helium gas plume produced by a pulsed gas jet backed with 50 bars of pressure (an estimated gas density of $\approx 5 \times 10^{18} \text{ cm}^{-3}$). High order harmonics with a plateau out to the 21st order were produced.

The coherence of these harmonics was measured by placing a slit pair 4 cm away from the gas jet plume and laser focus. These slit pairs were produced by laser drilling the slits in 20 μm thick Ti foil. Each slit had a width of $8 \pm 1 \mu\text{m}$ and slit pairs with spacings of 28, 50, 75, and 100 μm were used for the measurements. The harmonic radiation that traversed the slits was then spectrally dispersed with a grazing incidence, flat field spectrometer with a 50 μm entrance slit (oriented perpendicular to the slit pairs). The harmonics were detected with a CsI coated, dual microchannel plate detector. The total distance from the slit pair to the detector was 180 cm. This distance assured that the harmonic fringe spacing ($>600\text{--}1000 \mu\text{m}$) was larger than the estimated 100 μm spatial resolution of the detector. The harmonics' spatial profiles at the position of the double slits were measured by scanning a single, 8 μm slit across the profile. The spatial profiles were roughly Gaussian with a width of approximately 200 μm (full width at half maximum) at an intensity of $\sim 4 \times 10^{15} \text{ W/cm}^2$.

The coherence of a light source is typically characterized by its mutual intensity function [5], which can be frequently approximated as the product of the radiation intensity and the source complex coherence factor [12]. In an ideal double slit experiment, in which both slits are uniformly illuminated, the modulus of the

complex coherence factor is equal to the fringe visibility, defined as $V = (I_{\max} - I_{\min}) / (I_{\max} + I_{\min})$ [12], (where I_{\max} and I_{\min} are the maximum and minimum intensities of the fringe pattern). Thus we can directly derive information about the spatial coherence of the harmonics by measurement of the fringe visibility. Typical interference patterns obtained with slits with a $50 \mu\text{m}$ spacing centered on the harmonic beam are shown in Fig. 1(a). Here fringe patterns on the 11th to the 19th harmonic are shown (covering the wavelength range of 277 to 479 Å.) These data were taken with a peak laser intensity of $\sim 4 \times 10^{15} \text{ W/cm}^2$, an intensity above the ionization saturation intensity in helium ($\approx 1 \times 10^{15} \text{ W/cm}^2$). As illustrated in Fig. 1(a), all the harmonics exhibit interference fringes, though the fringe visibility is < 1.0 , indicative of partially coherent radiation.

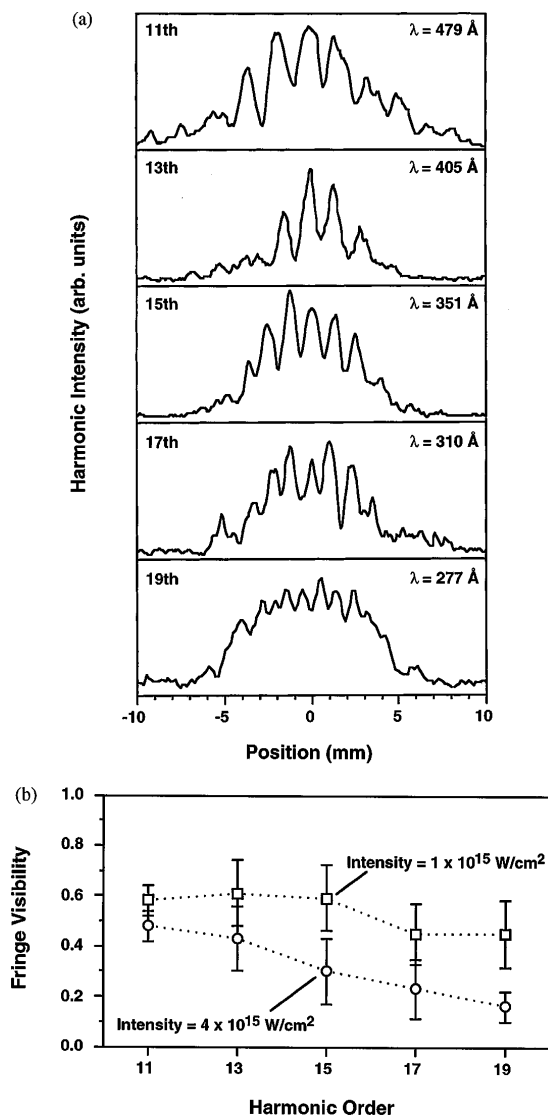


FIG. 1. (a) Typical interference patterns on the 11th to the 19th harmonic with a peak laser intensity of $\sim 4 \times 10^{15} \text{ W/cm}^2$ obtained with slits of $50 \mu\text{m}$ spacing centered on the harmonic beam. (b) Fringe visibility with a $50 \mu\text{m}$ slit spacing as a function of harmonic order.

In fact, the fringe visibility decreases with increasing harmonic order. Figure 1(b) shows the measured visibility with a $50 \mu\text{m}$ slit spacing as a function of harmonic order from the 11th to the 19th harmonic for two peak intensities, $1 \times 10^{15} \text{ W/cm}^2$ and $4 \times 10^{15} \text{ W/cm}^2$. Each point represents the average of six laser shots within a $\pm 10\%$ energy bin. The error bars in the measurement were determined by the extent of the shot to shot variation of the fringe visibility. For both intensities the fringe visibility slowly decreases with increasing harmonic order, though the fall is faster at the higher intensity.

Figure 1(b) also indicates that there is a variation in the harmonic fringe visibility with laser peak intensity. This effect is illustrated in Fig. 2(a) where the images and the resulting lineouts of the fringes from the 11th harmonic ($\lambda = 479 \text{ \AA}$) generated with slits of $50 \mu\text{m}$ separation are shown at two different peak intensities. The first shows the fringes generated with a peak intensity of $8 \times 10^{14} \text{ W/cm}^2$, below the onset of significant ionization in the helium gas. Here the fringes are sharp and well defined with a corresponding visibility of 0.8. In contrast, at the higher intensity of $5 \times 10^{15} \text{ W/cm}^2$, an intensity at which significant ionization has occurred in the helium, the fringes are broadened, with a drop in visibility to 0.45. Figure 2(b) illustrates the decrease in visibility for fringes of the 15th harmonic ($\lambda = 351 \text{ \AA}$) with $50 \mu\text{m}$ spaced slits as a function of intensity. Below the ionization saturation intensity the harmonic exhibits good fringe visibility (0.7–0.8). This visibility falls and levels off at about 0.4 at intensity above this value.

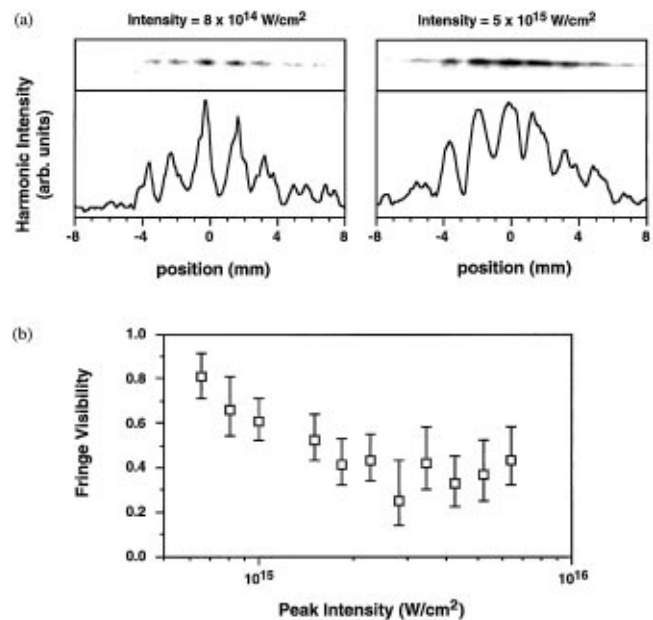


FIG. 2. (a) Images and lineouts of the fringes from the 11th harmonic ($\lambda = 479 \text{ \AA}$) generated with slits of $50 \mu\text{m}$ separation at two different peak intensities. (b) Fringe visibility of the 15th harmonic ($\lambda = 351 \text{ \AA}$) with $50 \mu\text{m}$ spaced slits as a function of peak laser intensity. (Each point represents the average of 3 to 5 laser shots.)

Despite this decrease of coherence with increasing laser intensity, we find that the spatial coherence of the harmonics is still high even at the high intensities. We can reconstruct the complex coherence factor and the effective coherence area of the harmonics by measuring the fringe visibility as a function of slit spacing [12]. Such measurements at an intensity of $4 \times 10^{15} \text{ W/cm}^2$ on the 13th harmonic ($\lambda = 405 \text{ \AA}$) and the 19th harmonic ($\lambda = 277 \text{ \AA}$) are shown in Fig. 3. (Inadequate spatial resolution precluded an accurate measurement of the visibility on the 19th harmonic with a $100 \mu\text{m}$ slit spacing.) From this measurement (which essentially gives the complex coherence factor $\mu(\Delta x, \Delta y)$ as a function of spacing Δx) we can use the van Cittert–Zernike theorem to estimate the effective coherence area A_c , given by $A_c = \int \int |\mu(\Delta x, \Delta y)| d\Delta x d\Delta y$ [12]. The coherence area can then be related to an effective incoherent source size $d_s = 2\lambda z / (\pi A_c)^{1/2}$. (This is the diameter of a uniform, incoherent source which yields the same coherence area as that measured. Thus a smaller effective source size indicates higher coherence.) Here z is the distance from source to slits. Assuming an azimuthally symmetric coherence function, an integration of the measured complex coherence factors indicates that the 13th and 19th harmonics exhibit effective incoherent source diameters of 15 and $16 \mu\text{m}$, respectively.

For comparison, the modulus of the complex coherence factor of a uniform incoherent disk emitting radiation at a wavelength of 405 \AA located at the laser focus with a diameter of $15 \mu\text{m}$ calculated using the van Cittert–Zernike theorem [12] is plotted on the data for the 13th harmonic and a similar plot for a 277 \AA source with a

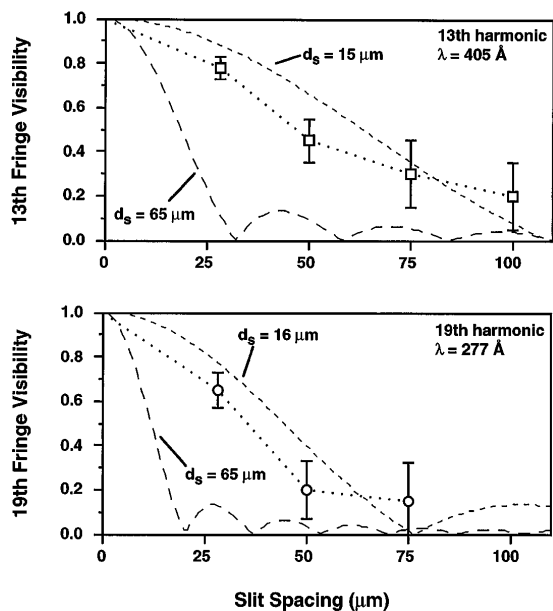


FIG. 3. Fringe visibility as a function of slit spacing with a peak intensity of $4 \times 10^{15} \text{ W/cm}^2$ for the 13th (top) and the 19th (bottom) harmonics. (Each point is a six shot average.) The dashed curves are the equivalent calculated visibility for incoherent disks.

diameter of $16 \mu\text{m}$ is compared to the data for the 19th harmonic. Clearly this simple model gives a reasonable estimation for the observed character of the complex coherence factor. The calculated coherence factor of a $65 \mu\text{m}$ source is also shown on these data in Fig. 3. $65 \mu\text{m}$ is the estimated size of the harmonic emission exiting the gas medium as calculated by a numerical solution of the wave equation for the 13th harmonic [13]. Our calculations indicate that the actual harmonic source size is, in fact, roughly equal to the laser spot source size ($\sim 70 \mu\text{m}$, $1/e^2$ diameter) despite the nonlinearity of the harmonic generation process because the harmonic yield is strongly saturated in the center of the Gaussian focus profile. The comparison in Fig. 3 clearly indicates that the observed harmonic's coherence is significantly better than a purely incoherent $65 \mu\text{m}$ source of radiation produced at the laser focus, consistent with the parametric nature of the harmonic generation process.

The observed partial degradation of coherence at high laser intensity is, according to the data of Fig. 2, correlated with the onset of ionization in the helium. This seems to indicate that the formation of a plasma by ionization is the primary cause of the observed decrease in coherence. The coherence of the harmonics can be degraded if a rapidly varying phase is imparted to the radiation, provided that this temporal phase variation is not the same at all points in the laser beam [12]. The rapid formation of free electrons during the harmonic generation will impart a rapidly varying phase on the harmonic, and this will lower the spatial coherence of the harmonics if the rate of formation of free electrons varies at different points in the beam. Variations in the initial gas density, for example, can provide the spatial nonuniformities required to degrade the coherence.

It is possible to make a simple estimate of the effects of electron density fluctuations on the coherence of the harmonic radiation by considering the production of harmonics by a collimated laser plane wave (a good approximation in our experiment since we use a weak focus). The harmonic field is $A_q(t) \cong -2i\pi k_q n_0 l [d_q[A_0(\mathbf{x}, t)]] \text{sinc}[\Delta k l / 2] e^{-i\Delta k l / 2}$ in this approximation [1], where the phase mismatch is determined by the free electron density $\Delta k \approx (\pi q / \lambda_0) (n_e / n_{\text{crit}})$ (here n_{crit} is the laser critical density, equal to $4 \times 10^{21} \text{ cm}^{-3}$ for 527 nm light, and l is the medium length $\approx 2 \text{ mm}$ in our jet). The complex coherence factor for the harmonic radiation is given by [12]

$$\mu_{12} = \frac{\langle A_q(\mathbf{x}_1, t) A_q^*(\mathbf{x}_2, t) \rangle}{\sqrt{\langle A_q(\mathbf{x}_1, t) A_q^*(\mathbf{x}_1, t) \rangle \langle A_q(\mathbf{x}_2, t) A_q^*(\mathbf{x}_2, t) \rangle}}, \quad (1)$$

where the angle brackets denote an appropriate time average (an average over the entire harmonic pulse in our case). We can derive a simple scaling for the complex coherence factor if we assume that the harmonic pulse is square in time and that the electron density ramps up linearly over the harmonic pulse. If the linearly increasing electron

density between points \mathbf{x}_1 and \mathbf{x}_2 differs by the amount δn_e at the end of the pulse then the complex coherence factor is

$$|\mu_{12}| = \left| \text{sinc} \left[\frac{\pi q l}{4 \lambda_0 n_{\text{crit}}} \delta n_e \right] \right|. \quad (2)$$

The maximum electron density at which harmonics will be produced is that at which $\Delta k l \sim 2\pi$, implying a maximum electron density of roughly $(1-5) \times 10^{17} \text{ cm}^{-3}$ for the harmonics we have studied. It is reasonable, therefore, to assume that the electron density can fluctuate by an amount that is comparable to this value. Equation (2) implies that electron density variations of this magnitude will degrade the coherence to $\mu \sim 0.9-0.6$, roughly comparable to the measured coherence of the harmonics. Equation (2) also implies that the coherence will be degraded as q increases, consistent with the data shown in Fig. 1(b).

To further illustrate this point we have performed numerical calculations to derive the harmonic field in the presence of initial gas density variations. This model involves solving the wave equation for the harmonic field in the presence of ionization and has been described previously in detail [13]. For illustrative purposes the calculated complex coherence factor of the 15th harmonic as it exits the medium as a function of spacing is shown in Fig. 4 for two intensities. This calculation assumes a 1 ps, 527 nm pulse in 1 mm of helium gas with a mean density of $5 \times 10^{18} \text{ cm}^{-3}$. A 30% initial density ramp is placed across the $70 \mu\text{m}$ Gaussian focal spot in one spatial direction. (This density profile is chosen for illustrative purposes only, but it is not unreasonable to assume that gas density variations of this order can occur across the profile of the gas jet output at the high backing pressure used in our experiment [14].) As shown in Fig. 4, with a peak intensity of $5 \times 10^{14} \text{ W/cm}^2$ the harmonic exhibits near perfect coherence across the beam. At an intensity of $3 \times 10^{15} \text{ W/cm}^2$ the coherence is clearly degraded.

Though the calculated coherence factor does not exactly match the observed decrease in coherence we emphasize that this calculation is meant only for qualitative estimates. For example, our model does not include such effects as

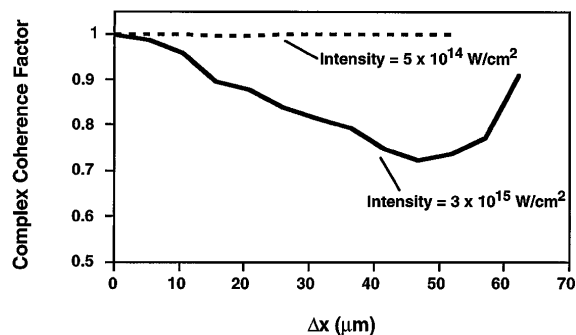


FIG. 4. Calculated complex coherence factor of the 15th harmonic as it exits the medium as a function of spacing for two peak intensities.

laser beam refraction and filamentation in the plasma, effects which are, in general, difficult to model accurately. Such refraction effects can effect the harmonics' far field profiles [15] and can further degrade the harmonics' coherence. Nonetheless, it is clear from this analysis that spatial nonuniformities in the free electron formation can have a dramatic effect on the spatial coherence of the harmonics.

In conclusion, we have presented the first measurement of the spatial coherence of the high order harmonic radiation in the soft x-ray region of 270–480 Å. We find that the harmonics exhibit good coherence, even at high intensity, though the coherence is degraded by the onset of field ionization in the medium. The magnitude of the coherence degradation is consistent with some simple estimates and harmonic production calculations in the presence of density variations. We find that the harmonics exhibit an effective incoherent source size that is approximately $15 \mu\text{m}$ in diameter. These coherence characteristics are substantially superior to those of previously reported measurements of x-ray laser coherence, which typically exhibit an effective coherence source size of $\sim 100 \mu\text{m}$ [7,10]. Thus the coherence area of the harmonics is nearly 2 orders of magnitude larger than soft x-ray lasers.

We acknowledge financial support by the UK EPSRC and the Ministry of Defense. D.D.M. acknowledges travel support from NATO Contract No. CRG 930274.

-
- [1] A. L'Huillier, L. Lompré, G. Mainfray, and C. Manus, in *Atoms in Intense Laser Fields*, edited by M. Gavrila (Academic Press, Boston, 1992), pp. 139–202.
 - [2] J.W.G. Tisch, R.A. Smith, J.E. Muffett, M. Ciarrocca, J.P. Marangos, and M.H.R. Hutchinson, *Phys. Rev. A* **49**, R28 (1994).
 - [3] P. Salières, T. Ditmire, K.S. Budil, M.D. Perry, and A. L'Huillier, *J. Phys. B* **27**, L217 (1994).
 - [4] J. Peatross and D.D. Meyerhofer, *Phys. Rev. A* **51**, R946 (1995).
 - [5] M. Born and E. Wolf, *Principles of Optics: Electromagnetic Theory of Propagation Interference and Diffraction of Light* (Pergamon Press, Oxford, 1980).
 - [6] M.H. Sher, S.J. Benerofe, J.F. Young, and S.E. Harris, *J. Opt. Soc. Am. B* **8**, 114 (1991).
 - [7] J.E. Trebes *et al.*, *Phys. Rev. Lett.* **68**, 588 (1992).
 - [8] I.C.E. Turcu *et al.*, *J. Appl. Phys.* **73**, 8081 (1993).
 - [9] P. Salières, A.L. Huillier, and M. Lewenstein, *Phys. Rev. Lett.* **74**, 3776 (1995).
 - [10] P. Celliers, F. Weber, L.B. DaSilva, J.T.W. Barbee, R. Cauble, A.S. Wan, and J.C. Moreno, *Opt. Lett.* **20**, 1907 (1995).
 - [11] T. Ditmire, J.K. Crane, H. Nguyen, L.B. DaSilva, and M.D. Perry, *Phys. Rev. A* **51**, R902 (1995).
 - [12] J.W. Goodman, *Statistical Optics* (John Wiley & Sons, New York, 1985).
 - [13] T. Ditmire, K. Kulander, J.K. Crane, H. Nguyen, and M.D. Perry, *J. Opt. Soc. Am. B* **13**, 406 (1996).
 - [14] C. Altucci *et al.*, *J. Phys. D* **29**, 68 (1996).
 - [15] T. Ditmire, J.K. Crane, H. Nguyen, and M.D. Perry, *J. Nonlinear Opt. Phys. Mat.* **4**, 737 (1995).